Int. J. Electrochem. Sci., 7 **(2012)** 4121 - 4132

International Journal of
ELECTROCHEMICAL
SCIENCE
www.electrochemsci.org

Characterization of Passive Films Formed on Manganese Nickel-Free Stainless Steel Exposed to Simulated Concrete Pore Environment

L. Veleva[1,*], *B. Tsaneva*[2], *P. Castro-Borges*[1] *and M.Burova*[3]

[1] Department of Applied Physics, CINVESTAV-IPN, 97310, Merida, Mexico
[2] Department of Chemistry, Technical University of Sofia, Sofia 1756, Bulgaria
[3] Sofia University, Faculty of Physics, Department of Physics of Semiconductors, Sofia, Bulgaria
[*]E-mail: veleva@mda.cinvestav.mx

Received: 27 March 2012 / *Accepted:* 19 April 2012 / *Published:* 1 May 2012

Manganese is a key component in low-cost SS formulations when nickel is replaced by Mn. Passive layers grown on Cr18Mn12 free-nickel SS samples after immersion in saturated $Ca(OH)_2$ and Portland cement extract test solutions, containing different chloride additions, were studied. The corrosion behavior of the passive films was monitored at open circuit potential in both alkaline solutions. In the presence of chloride ions the passivation process is perturbed and competes with the dissolution one. The surface becomes irregular, rough and Mn was found enriched in areas of non metallic inclusions in the passive layer, while the Fe/Mn and Fe/Cr ratios tend to decrease. The formed film is N-richer at the metal-oxide interface, as a consequence of its anodic segregation during dissolution-passivation process. Surface protuberances in the morphology of the SS could be explained in terms of unattacked oxide inclusions that still remain in the formed passive film or due to manganese insoluble compounds, which aid the corrosion resistance of the studied steel.

Keywords: Corrosion, Simulated concrete, Chlorides ions, Stainless steel, Passive film

1. INTRODUCTION

Concrete reinforced structures are usually very resistant to corrosion phenomena, because the alkaline concrete environment (pH 12 -/13) passivates the steel by the formation of an iron oxide/hydroxide layer [1]. However, the reinforced concrete can deteriorate when voluminous corrosion products are formed on the steel surface, even when a high pH in the concrete is maintained, due to the presence of Cl^- ions and moisture that can lead to pitting corrosion and breakdown of the grown passive layer. Carbon (mild) steel is the primary metal used for reinforced concrete, however,

interest in the use of austenitic stainless steel (SS) has appeared, to assure higher durability of structure exposed to aggressive environment [2]. The interest in SS is a result of its resistance to a great variety of environments and its property of self-regeneration after partial destruction of its passive film. Attempts have been made to develop austenitic stainless steel with replacement of nickel with other cheaper austenite stabilizers such as manganese (Mn), to decrease the SS cost. Manganese is a key component in low-cost SS formulations, which may contain up to 16% Mn, when nickel is replaced in part or entirely by Mn (nickel-free SS). But Mn is not as effective austenitic stabilizer as Ni, and this problem can be solved by combining Mn with nitrogen (N) in these SS alloys. Nitrogen also improves resistance to localized corrosion, and has several other benefits such as increased strengthening and retardation of sensitization [3-7]. It is known for the manganese detrimental effect on the pitting corrosion resistance, associated with the formation of non-metallic Mn type of inclusions, which could serve as initiation sites for localized pitting corrosion, but it has been found that the growth of stable pits only occurs close to inclusions with sizes above 0.7 μm [8-10]. Three types of inclusions have been described: MnS, multielement (Cr, Mn) oxides, and mixtures of sulfides and oxides, stating that the multielement oxide inclusions either did not initiate pits or initiated small corrosion sites which repassivated before significant dissolution occurred.

One of the nickel-free SS, considered as possible cheap alternative, that could substitute the conventional Cr-Ni SS (AISI 304), is the steel Cr18Mn12N. Its well-balanced chemical composition preserves the SS austenitic structure formation, as does nickel, and allows a suitable thermal treating, without lowering the Cr percentage. This SS (nickel-free) is considered as high nitrogen alloyed austenitic steel (HNS), because its nitrogen content (0.61 wt/%) exceeds 0.4 wt.%. Because of their many different excellent properties HNSs are finding applications in several branches of industry, almost always requiring high corrosion resistance.

The present work aimed to study the corrosion behavior of Cr18Mn12N stainless steel samples, after their exposure to a Portland cement extract solution that simulates concrete pore environment, in presence and absence of NaCl. An attempt was also made to correlate the passive film composition (SEM-EDX) and topography (AFM) with SS behavior. Studies of steel corrosion in reinforced concrete are principally concerned with the behavior of carbon steel, and the information about stainless steel in alkaline media, and especially in CE solutions, is scarce. Besides, researches and proposed mechanisms, related with manganese SS corrosion behavior, have been referred mainly to tests in acid environments.

2. EXPERIMENTAL

Cement paste hydration mainly involves the reaction of Ca_3SiO_5 (or $3CaO.SiO_2$), Ca_2SiO_4 (or $2CaO.SiO_2$), and other calcium containing minerals with free water to form $Ca(OH)_2$ (~/30%), calcium silicate hydrate ($CaO.2SiO_2.4H_2O$), and an amorphous gel containing several ions (e.g. Al^{3+}, Fe^{3+}, SO_4^{2-}). The alkaline $Ca(OH)_2$ containing solution remains in the pores of the hydrated cement during its curing process. This solution has a large buffer capacity and acts as a diffusion barrier to corrosive agents to the metal surface [11]. Corrosion of reinforcing steel is governed principally by the

microstructure of the solid cement phase, the aggressiveness of the electrolyte (Cl^-) inside the concrete pores, and the microstructure of the passive oxide layer formed on the steel. Corrosion of steel embedded in concrete is a subject of discussion regarding to instrumental techniques and data interpretation. Difficulties in experimental measurements include the electrode and cell designs (e.g. the position of the reference and counter electrode) [12], the large potential drop (IR) in concrete and its compensation, the development of macro-corrosion cell [13], the restriction of oxygen diffusion, etc. An alternative approach, which avoids many of the above difficulties, is to use electrodes immersed in model solutions that simulate the concrete pore solution environment. Model solutions allow one to obtain comparative results and the control of some parameters, which is difficult to accomplish in reinforced concrete samples. Many model solutions have been proposed, including the use of a saturated aqueous $Ca(OH)_2$ solution (pH 12-13) [14-17], aqueous KOH and NaOH [18-20] and cement extract (CE) solutions [16-21]. The most common model solution is saturated $Ca(OH)_2$, however, the real composition of concrete pore solution is complex, since it includes a number of other compounds besides $Ca(OH)_2$. In our previously reported studies two model solutions, saturated $Ca(OH)_2$ and CE solution both at pH 12.79 ±/0.2, in open air and at room temperature were used to simulate the corrosion behavior of mild steel and AISI 316 rebar in the concrete pore environment.

2.1. Samples and experimental solutions

Samples of Cr18Mn12N (nickel-free) stainless steel were prepared by cutting plate of 8 mm of diameter. The reported SS chemical composition is (wt.%): Cr 16.50, Mn 12.00, Si 0.30, N 0.61, C 0.04 and the balance Fe. The austenitic structure of this SS was obtained upon quenching in water after heating at 1100ºC. Oxides and oxide-sulphides were mainly detected as non-metallic inclusions in the steels. The surface samples were polished by grinding with 320, 600, 1500 and 2000 grit SiC paper. Two model solutions were prepared with distilled deionized water and analytical grade reagents: (a) saturated $Ca(OH)_2$ solution (pH=12.7) and (b) CE solution (pH=12.9). Solution (b) was prepared from 1:1 wt./wt. mixture of type I Portland cement (CEM I 42.5R, BDS EN 197-1) with water. The mixture was stored for 24 h and filtrated. All solutions were kept in closed containers before and after the immersion of steel samples. Steel passivation was studied in the absence of chlorides and also in their presence (0.5, 1.0, 3.0, 5.0 and 10.0% NaCl) at room temperature (20ºC). The reported free chloride threshold levels are in the range of 0.2 (1.6 %) to 1.8 M/L (10.4 %) of NaCl, or 0.1 to 6.0 [Cl-]:[OH-] ratio. For specific study cases, chloride threshold levels are close to 1.0 % by weight of concrete (23000 ppm of Cl^- in concrete) as can be observed in Figure 1. This threshold level was obtained after more than 60 years of exposure to the marine environment.

The open circuit potential (free corrosion potential) of the steel samples was measured during 24 hours in both experimental solutions, using GPHR 1400 Digital-pH/mV-Meter. The potentials are referred to the saturated calomel electrode (SCE).

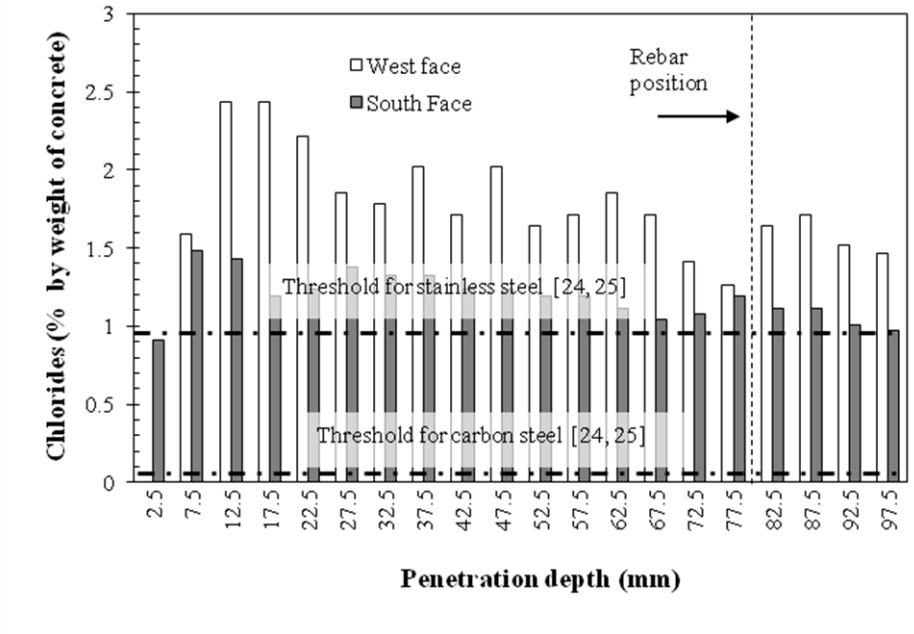

Figure 1. Chloride concentration profiles in the girder # 9

2.2 SEM-EDX, XRD and AFM analysis

Scanning Electron Microscope - Energy-Dispersive X-ray Spectroscopy (SEM-EDX, SEM Philips XL 30 ESEM TMP) was used to study the morphology and the elemental composition of the passive layers formed on SS samples. The SS samples were examined after 30 days of exposure in each model solution. The results were compared with those of the native passive film, produced in air (before an immersion in model solutions).

The austenitic steel structure of Cr18Mn12N SS was determined by means of X-ray diffraction analysis (Siemens D 5000 Diffractometer, with CuKα monochromatic radiation, λ = 1.5418 Å), using Bragg-Brentano geometry (10 seg/0.02º, tube voltage of 30 kV and a current of 20 mA). Samples were mounted with a beam incidence angle of 1º and detector scan rate of 2º /min.

The dimensional characterization of the formed passive films was conducted by means of atomic force microscope (AFM), Anfatec Instruments AG of Germany, with a resolution of 0.45 nm in X and Y at a scanning area of 30x30 micrometers and 0.078 nm in Z. A silicon nitride coated tip was used, with a radius of curvature of 10 nm. The samples were scanned in about 512 points in the X and Y axes, representing each an area of interest. MatLab software statistics was used for Gauss curve fitting, mean roughness (Ra) and root mean square characterization of SS samples surface.

3. RESULTS AND DISCUSSION

3.1 Open circuit potential

Series of open circuit (free corrosion) potential (o.c.p) values were acquired at Cr18Mn12N SS samples (electrodes), during their immersion in both model solutions, and the oxide film was allowed

to form without external polarization (Figure 2). Starting from negative value of -450 mV *vs* SCE, corresponding to the native formed passive film on the steel in air, the SS surface tended to additional passivation in the alkaline solutions and the o.c.p. shifted to more positive values. In cement extract solution (CE) the anodic displacement is gradual and in 25 h the formed passive film stabilizes, presenting 180 mV more positive o.c.p. value. In saturated $Ca(OH)_2$ solution the gradual anodic shift of o.c.p. as a function of time is not observed: in the first 5 h it tends to a more positive value and after that period its returns to less noble potentials (lower anodic polarization). This fact suggests that in this model solution the formed passive layer on Cr18Mn12N surface is different and probably having lower corrosion resistance, then the passive one grown in CE model solution.

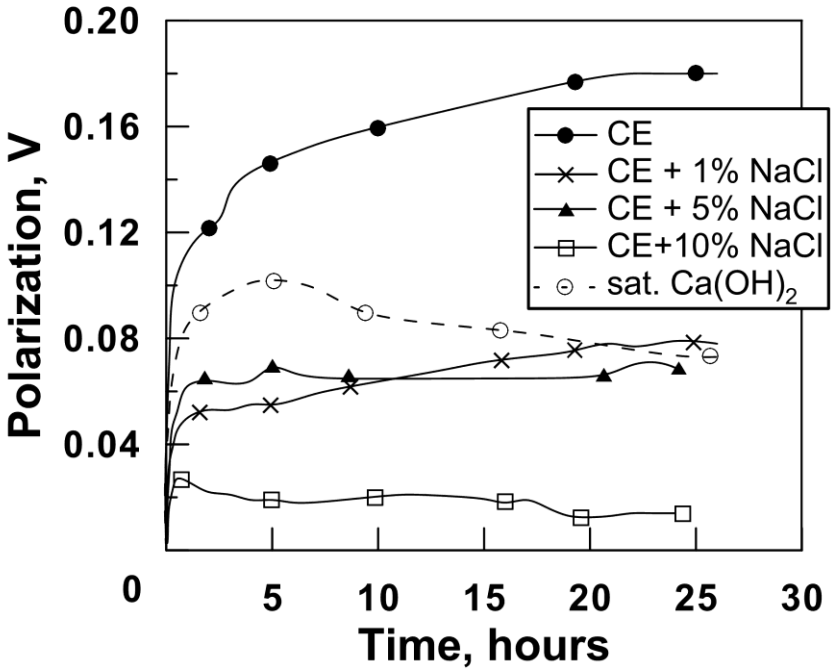

Figure 2. Anodic displacement (polarization) of the initial o.c.p. values of Cr18Mn12N samples, exposed to alkaline solutions at 20ºC, as a function of time: saturated $Ca(OH)_2$; cement extract (CE); CE + 1%, 5% and 10% wt NaCl.

It can be seen that when the SS surface is submitted to aggressive chloride ions attack, in CE solution steel passivation process cannot be completed and the anodic polarization tendency is less pronounced (Figure 2). The influence of chloride concentration on the measured steady state values of o.c.p. is shown in Figure 3. The results indicate that the presence of chloride ions and increase of their concentration are very critical for the stability of initially grown passive layer on the steel surface in absence of chloride. In cement extract solution (CE), where the o.c.p. reached more positive potential in absence of chloride (-0.270 V), the passive layer still maintains more noble potentials, compared to those in saturated $Ca(OH)_2$. In the region of critical concentration (0.5 – 1.0% NaCl) for the initiation of steel corrosion in concrete (CE), the studied SS is well resistant (Figure 3). The o.c.p. potentials shift to more negative values that reach at 10% NaCl approximately the initial o.c.p. (-450 mV), which

corresponds to the formed oxide layer in air, before SS exposure to CE solution. This tendency is not apparent for samples in $Ca(OH)_2$ (Figure 3), due to the fact that o.c.p. in an absence of chloride showed very poor tendency for anodic passivation (Figure 2).

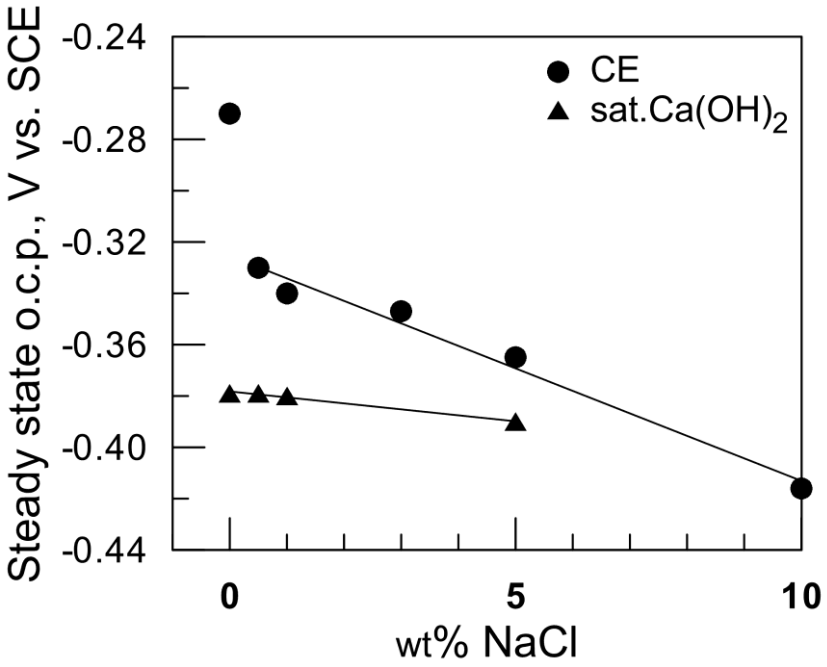

Figure 3. Values of o.c.p. of Cr18Mn12N samples after 24 h exposure to CE-extract and sat.Ca(OH)2 alkaline solutions, as a function of chloride concentration: 0.0; 0.5; 1.0; 3.0; 5.0 and 10% NaCl (20ºC).

Corrosion and passivation of stainless steels in alkaline solutions are relatively complex processes that are not yet fully understood because the composition and structure of the passive layer is still incompletely. This is partly because the passive films are so thin and because the structure should ideally be studied in the wet electrochemical environment in which these films are formed. Giving these findings, we recommend also electrochemical study under o.c.p., when the passive layer is naturally formed, without external polarization. The composition of the passive layer (oxides or hydroxides) and its structure (crystalline or amorphous) remains controversial, despite the use of in situ and ex situ techniques [22, 23, 27].

3.2. Elemental chemical analysis of the surface of passive films formed on nickel-free SS

The passive films formed on stainless steel surface are of semiconducting nature, which exact electronic structure is not fully known. The passive layer has a duplex structure: an inner part (p-type semiconductor), mainly formed by chromium oxide, and an outer region (n-type), reach in iron oxide. SS passive layer breakdown is a very complex and it is not fully understood. The existing models [27] for SS breakdown are:

a) Local thinning of the passive film in aggressive (Cl^-) environments;

b) "Mechanical" or electrocapillary, or electrical breakdown of the passive film precedes local dissolution of the metal (pits formation);

c) Cl^- penetrates the passive film without destroying it; dissolution of metal occurs when Cl^- reaches the metal and its concentration is high enough.

Figure 4 presents defects observed on Cr18Mn12N surface samples, after 30 days of exposure in CE and sat. $Ca(OH)_2$ alkaline solutions, reported as black spots, white spots and white flakes, or areas where the passive film has not been formed or perturbed. SEM analysis reveals that the shining "white flakes" are areas of electrically charged surface, due to its low electronic conductivity. This fact corresponds to typical products, usually salts or non-metallic oxides, deposited on the surface, which properties are dielectric.

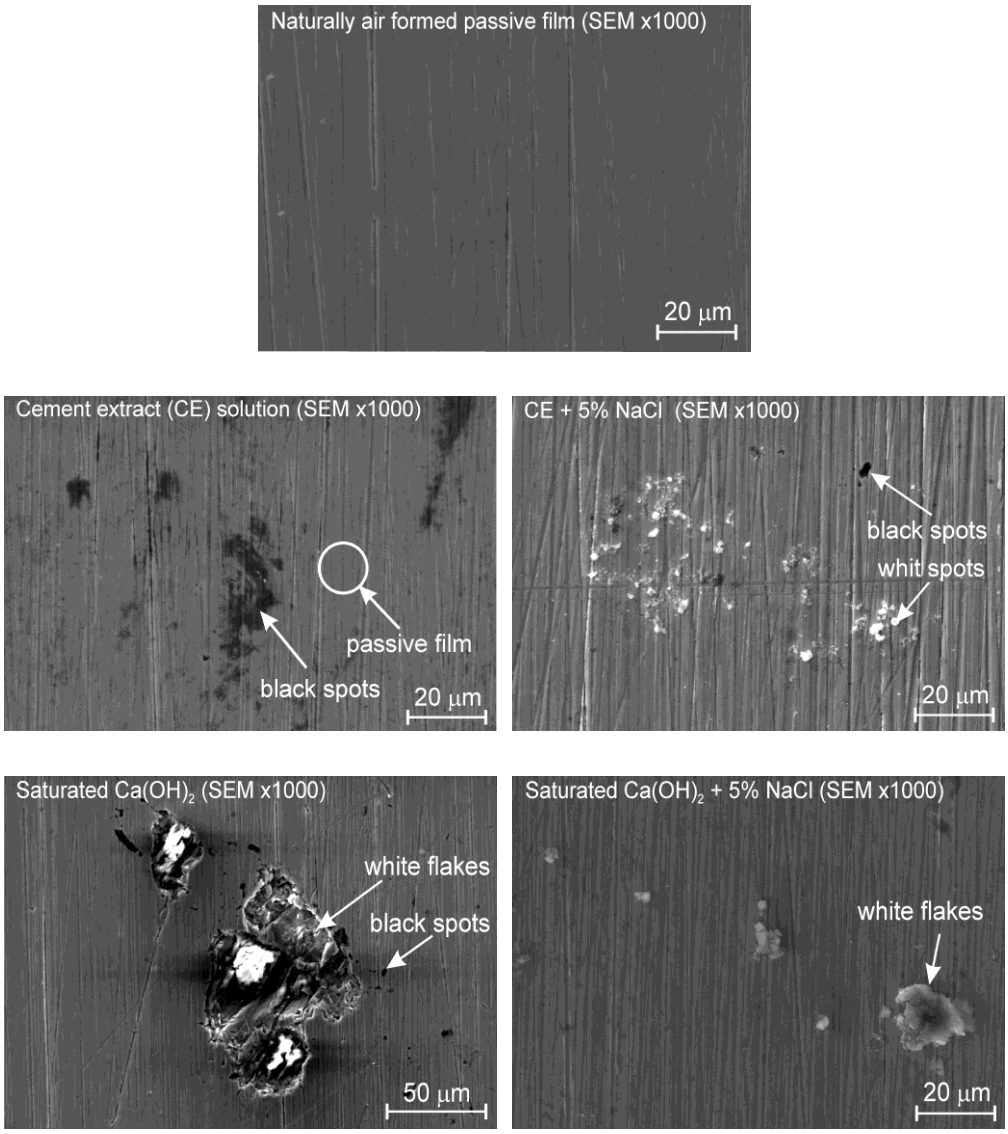

Figure 4. SEM images of defects observed on Cr18Mn12N surface after 30 days of exposure in CE and sat. Ca(OH)2 alkaline solutions, with the addition of 5% NaCl: black spots, white spots and white flakes, or areas where the passive film has not been formed or perturbed.

Table 1 report a resume of SEM-EDX elemental chemical composition of the surface of the passive films formed on Cr18Mn12N SS after 30 days of exposure in alkaline simulated concrete solutions. The results are compared to those of naturally air formed passive film as reference sample.

Table 1. Elemental chemical analysis (EDXA) of passive layers formed on Cr18Mn12N SS after 30 days of exposure in alkaline solutions (1-4), compared to naturally air formed passive film (Reference sample).

Solutions	Element (wt%)	O	Fe	Mn	Cr	C	N	Si	Ca
(1) CE	Passive film	3.8	61.6	11.2	17.5	2.7	2.5	0.7	-
	Black spots	4.1	58.6	10.7	16.8	6.8	2.6	0.4	-
(2) CE + 5% NaCl	Passive film	4.0	61.5	11.0	17.6	2.6	2.7	0.5	-
	Black spots	7.0	50.0	16.3	15.1	5.6	2.7	1.9	-
	White spots	4.8	58.5	10.5	16.8	5.8	2.5	0.5	0.5
(3) Ca(OH)2	Passive film	3.5	62.7	11.1	17.3	2.5	2.2	0.6	-
	Black spots	3.2	61.7	10.6	16.9	5.2	1.9	0.4	-
	White flakes	32.3	4.0	41.8	2.4	4.4	-	15.0	-
(4) Ca(OH)2 + 5% NaCl	Passive film	4.1	63.9	10.6	17.5	3.4	-	0.5	-
	White flakes	15.4	30.3	5.4	8.9	24.7	-	15.3	-
(5) Reference sample	Passive film	4.2	63.6	11.3	18.1	2.4	-	0.4	-
	Black spots	4.1	63.3	11.1	18.0	3.1	-	0.5	-

The elemental chemical analysis revealed several events:

- Manganese (Mn) was found enriched in areas of defects of the passive layers. Its segregation could be explained in terms of diffusion. According to reports, the multielement (Cr, Mn) oxides inclusions either do not initiate pits or initiate small corrosion sites which repassivate before significant dissolution occurred [10].
- Nitrogen (N) does not take part as an element of the passive film formed at open air (Reference sample). However, in both highly pH alkaline solutions the passive oxide films become N-richer (2.5 – 2.7 wt.%) as a consequence of its anodic segregation during dissolution-passivation process and it is probably bonded more to Cr and not to Mn [28, 29].
- Surface defects, such as "white flakes", formed in saturated $Ca(OH)_2$, showed lower enrichment in Cr and Fe, which may be directly related to chromium and iron oxides. This result indicates a worse corrosion behavior of the studied steel in this model solution.
- The ratios Fe/Mn (6.0) and Fe/Cr (3.5) of the native (air) passive film seem to be maintained relatively in the same order in alkaline solutions. However, in the areas of defects (black spots or white flakes) these ratios tend to decrease. The chloride ions do not participate in the passive film structure under the experimental conditions tested.

- The black spots are abundant in carbon or carbides, which inclusions perturb the formation of homogeneous passive layer on the SS surface.

3.3. Topography of passive films formed on nickel-free SS

More than 18 AFM images of samples were processed and the results indicated that the film surface protuberances are in 25-20 nm higher that the surrounding areas, except few of them that reached 50 nm of height. AFM images revealed that in CE solution, the additionally formed passive layer shows less protuberances and the surface becomes more homogeneous, with lower h/w/l ratios (Figure 5: 1), compared to those of air formed passive film (Figure 5: 5). The passive layer roughness increased when the SS was immersed in saturated $Ca(OH)_2$ solution (Figure 5: 3). In the presence of the aggressive chloride ions (5% NaCl) the competing corrosion and passivation processes aid to changes in the SS relieve and it becomes irregular, rough and less homogeneous (Figure 5: 2, 4). These images indicate that SS corrosion dissolution (at non-metallic inclusion boundaries and scratches) proceeds, and this fact is more pronounced in saturated $Ca(OH)_2$ solution (Figure 5: 4). The observed corrosion attack, due to the presence of aggressive chloride ions, should not be considered as a pitting formed in the passive layer, because the critical pitting potential of the studied SS is about +100 mV (vs SCE), measured in 3.5% NaCl solution (pH=12), and the reported above o.c.p. values (Figures 2-3) are more negative. However, in alkaline solutions the chloride ions could attack passive steel areas (anodic sites) in the vicinity of non-metallic inclusions (cathodic sites) and pH of those corroded sites increases, giving possibility for a new consecutive dissolution of SS surface. Sticking out particles observed on the surface could indicate corrosion products, which probably accumulate over cavities. Such kind of protuberances, observed by AFM on 316 SS have been explained in terms of unattacked oxide inclusions that still remain on the SS surface in the formed passive film [30]. Another possibility is that the manganese tends to form insoluble compounds in alkaline environment and this fact aid the corrosion resistance of the studied Ni-free manganese stainless steel.

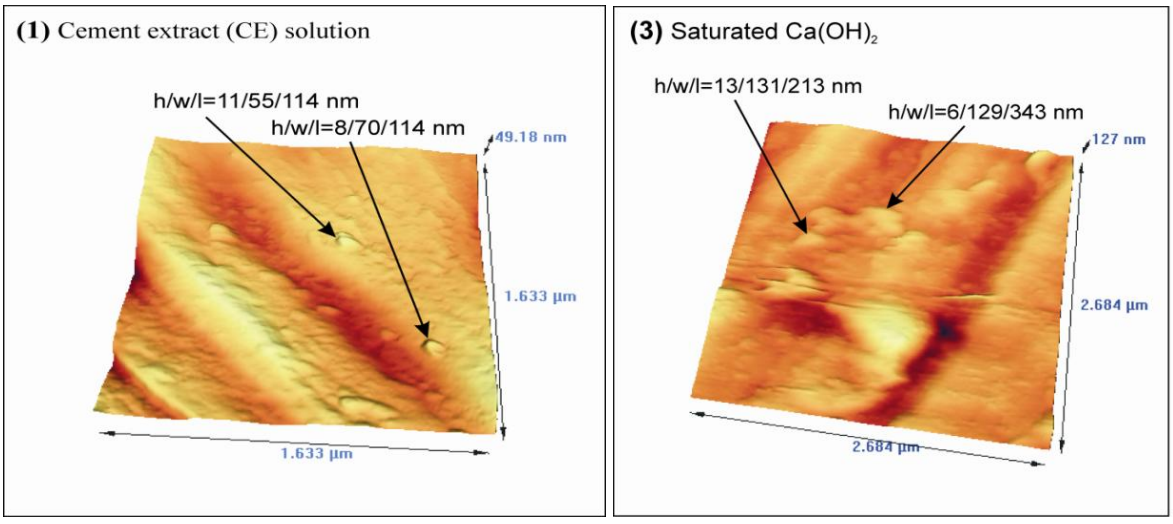

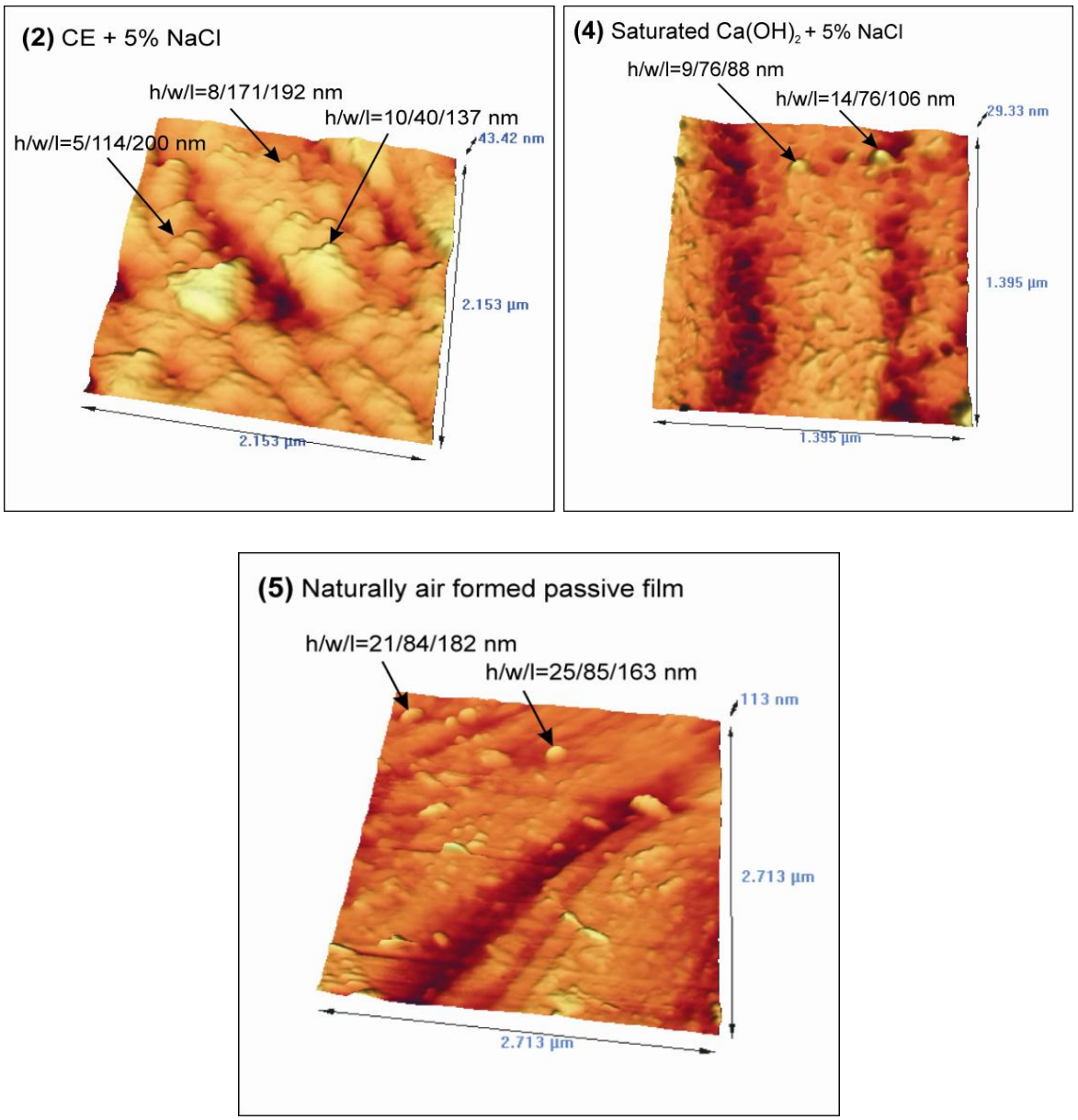

Figure 5. Topography (AFM) images of passive layers formed on Cr18Mn12N SS samples after 5 day exposure in: (1-2) CE; (2-3) saturated Ca(OH)2; (5) naturally air formed passive film-reference sample.

3.4. XRD-analysis of Cr18Mn12H SS

XRD patterns of all samples of Cr18Mn12N SS, shown in Figure 6, revealed that there was no phase changes induced after exposure of SS samples to both alkaline model solutions. The registered XRD patterns showed characteristic refraction indexes of austenitic AISI 304 structure. The relatively strong and narrow peak (at 44.2) manifests that the SS has a predominant crystalline structure. It is typical for crystalline orientation (111) on austenitic SS 304. A little displacement of some indexes is probably due to the replacement of Ni by Mn and N in the studied SS. There were not detected differences in XRD patterns of samples exposed to both alkaline solutions, even in the presence of

chlorides. Their XRD patterns coincide with those of air formed passive film (reference sample).

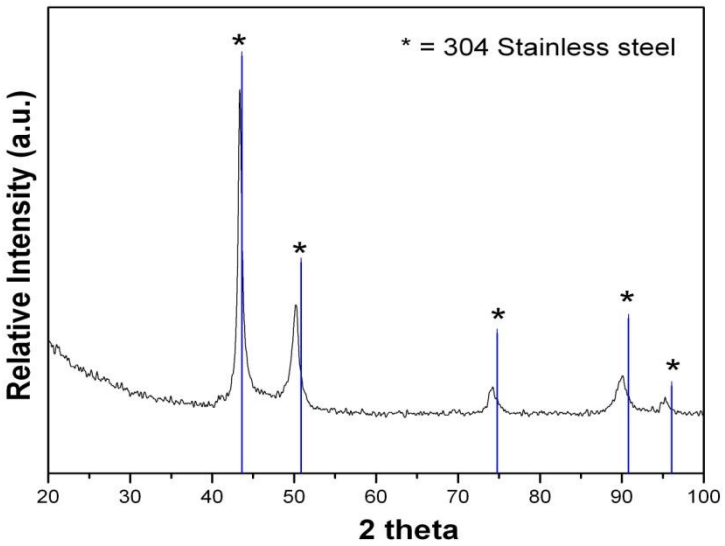

Figure 6. XRD scans conducted on the passive films of SS Cr18Mn12N formed in air and after exposure in alkaline solutions (saturated Ca(OH)2 and CE extract).

4. CONCLUSIONS

The corrosion behavior of Ni-free manganese stainless steel Cr18Mn12N was studied at open circuit potential (free corrosion potential) in two alkaline solutions, which simulate concrete pore environment: cement extract and saturated $Ca(OH)_2$. The results of these experiments support the following conclusions:

1) In a presence of chloride ions the passivation-repassivation process is perturbed and competes with the dissolution processes, which occurs on areas of surface defects. AFM images demonstrate that in the presence of chloride aggressive ions the SS relieve becomes irregular, rough and less homogeneous.

2) Sticking out particles observed on the surface could indicate corrosion products, which probably accumulate over cavities. Such kind of protuberances could be explained in terms of unattacked oxide inclusions that still remain on the SS surface in the formed passive film or due to manganese insoluble compounds, which aid the corrosion resistance. The corrosion attack, due to the presence of aggressive chloride ions, should not be considered as a pitting formed in the passive layer, because the critical pitting potential of the studied SS is more positive, compared to the reported o.c.p. in this study.

3) Manganese was found enriched in areas of defects of the passive layer, formed in alkaline solutions, while the ratios Fe/Mn and Fe/Cr tend to decrease. Nitrogen does not take part as an element of the passive film formed at open air. The chloride ions do not participate in the passive film structure.

4) A more resistant passive layer is formed in CE extract, probably due to its distinctive composition, homogeneity and thickness. The used alkaline solutions simulate the concrete pore environment in a different way.

ACKNOWLEDGMENTS
The authors express their thanks to Institute of Metal Science at Bulgarian Academy of Science for the supply of stainless steel samples and to CINVESTAV-Merida, Applied Physics Department, for the financial support of this study. The authors acknowledge the support of M. Balancan for her assistance.

References

1. M. Pourbaix, *Atlas of Electrochemical Equilibria in Aqueous Solutions*, NACE-CEBELCOR, Houston, (1974).
2. B. G. Callaghan, Corros. Sci., 35 (1993) 1535
3. V.A. Sadough, J. P. Audouard and P. Marcus, *Corros. Sci*., 36 (1994) 1825
4. R. C. Newman and T. Shahrabi, *Corros. Sci***.,** 27 (1987) 27.
5. G. C. Palit, V. Kain and H. S. Gadiyar, *Corros. J.*, 49 (1993) 977.
6. Ch. M. Tseng, H. Y., Liou and W. T. Tsai, *Mater. Sci. Ang.*, 190 (2003) A 344.
7. R. L. Klueh, P. J. Maziasz and E. H. Lee, *Mater. Sci. Eng.*, 15 (1988) A 102.
8. R.A. Perren, T. A. Suter, P. J. Uggowitzer, L. Weber, R. Magdwoski, H. Böhni and M. O. Speidel, *Corros. Sci.*, 43 (2001) 707.
9. T. A. Suter, E. G. Webb, H. Böhni and R. C. Alkire, *J. Electrochem. Soc***.**, 148 (2001) B147.
10. R. R. Ke and R. Alkire, *J. Electrochem. Soc***.,** 139 (1992) 1573.
11. M. Nagayama and M. J. Cohen, *J. Electrochem. Soc.*, 110 (1963) 670.
12. M. Pech, A. Sagüés and P. Castro, *Corros. J.*, 54 (1998) 491.
13. P. Castro, E. Pazini, C. Andrade, C. Alonso, *Corros. NACE*, 59 (2003) 535.
14. J. L. Dawson, P. E. Langford, *The Use of Synthetic Environment for Corrosion Testing,* ASTM STOP 970, Ed. by P. E. Francis, T. S. Lee, Philadelphia (1988) 264.
15. T. Henriques, A. Reguengos, L. Proença, E. V. Pereira, M. M. Rocha, M. M. M. Neto and I. T. E. Fonseca, *J. Appl. Electrochem.*, 40 (2010) 99.
16. L. Veleva, M. A. Alpuche, M. B. Graves and D. Wipf, *J. Electroanalyt. Chem.*, 537 (2002) 85.
17. L. Veleva, M. A. Alpuche, M. B. Graves and D. Wipf, *J. Electroanalyt. Chem.*, 578 (2005) 45.
18. H. A. Berman, *Report No. FHWA-RD-74-1*,Washington: Federal Highway Administration (1974).
19. T. Zakroczymski, C. J. Fan and Z. Szklarska-Smialowska, *J. Electrochem. Soc*., 132 (1985) 2
20. S. Muralidharan, V. Saraswathy, K. Thangavel and S. Srinivasan, *J. Appl. Electrochem.*, 30 (2000) 1255
21. M. F. Montemor, and A. M. P. Simoes, *Electrochem. Acta*, 13 (1995) 453.
22. M. P. Ryan, M. F. Toney, A. J. Davenport, L. J. Oblonsky, *MRS Bull.*, 24 (1999) 29.
23. O.A. Albani, J. O. Zerbino, J. R. Vilche and A. J. Arvia, *Electrochem. Acta*, 31 (1986) 1403.
24. F. Cui and A. Sagüés, *Corros. NACE*, (2001) 01645
25. D. McDonald, M. Sherman, D. Pfeiffer, and P. Virmani, 17 (1995) 65.
26. P. Castro, *Third International Conference on Concrete under Severe Environments*, Eds. by N. Banthia, K. Sakai, O. Gjørv, Canada: (2001) 151.
27. Z. Sklarska-Smialowska, *Corros. Sci.*, 44 (2002) 1143.
28. Y.C. Lu, R. Bandy, C. R. Clayton and R. C. Newman, *J. Electrochem. Soc.*, 130 (1983) 1774.
29. A.S. Vanini, J. P. Audouard and P. Marcus, *Corros. Sci.*, 36 (1994) 1825.
30. U. K. Mudali and Y. Katada, *Elchem. Acta*, 46 (2001) 3735.